Electronic Supplementary Material (ESI) for RSC Advances.

Single-Walled Carbon Nanotube Composite Inks for Printed Gas Sensors: Enhanced Detection of NO_2, NH_3, EtOH and Acetone - Supplementary Information

Gwyn. P. Evans,[†] David. J. Buckley,[‡] Neal. T. Skipper,[‡] and Ivan. P. Parkin[*,¶]

E-mail: i.p.parkin@ucl.ac.uk

Phone: +44 (0)20 7679 4669. Fax: +44 (0)20 7679 7463

Additional Raman spectroscopy data is available for the materials used in synthesis and at various stages of the of the SWNT - metal oxide composite fabrication process (Fig. S1 to Fig. S5) . The characteristic peaks associated with HiPco carbon nanotubes are displayed,[1] along with those corresponding to the admixture materials. TGA data is supplied to show the mass change of HiPco SWNT material, metal oxides, the ESL Vehicle and the composite material as a function of temperature up to 800°C (Fig. S6 to Fig. S10).

X-ray diffraction for each sample was measured on a Panalytical XPert θ-θ powder diffractometer operated in Bragg-Brentano reflection geometry, Cu K_α X-rays ($\lambda = 1.5418$ Å) generated at 40 kV and 40 mA. Programmable divergence and anti-scatter slits were used to

*To whom correspondence should be addressed

[†]Dept.of Security and Crime Science, University College London, 35 Tavistock Sq., London, WC1H 9EZ, UK

[‡]London Centre for Nanotechnology and Department of Physics and Astronomy, University College London, Gower Street, London WC1E 6BT, U.K

[¶]Dept. of Chemistry, University College London, 20 Gordon St., London, WC1H 0AJ, UK

illuminate a 10 x 10 mm area of the powder surface, with a 0.1 mm receiving slit followed by a scattered beam curved graphite monochromator. Alignment linearity was checked by reference to a silicon standard, and instrumental resolution was measured via the *(00l)* reflections from a mica crystal. The measured full-width half-maximum (FWHM) for these mica peaks is $\Delta 2\theta \approx 0.015^\circ$ ($\Delta\theta/\theta \approx 0.001$) in the region of interest. Bragg peaks were fitted to the pseudo-Voigt 1 line shape:

$$\mathrm{I} = \mathrm{I_0} + \mathrm{A}\left\{\frac{2\mu}{\pi}.\frac{\mathrm{w}}{4(\mathrm{x}-\mathrm{x_0})^2+\mathrm{w}^2} + (1-\mu)\frac{\sqrt{4\ln 2}}{\sqrt{\pi}\mathrm{w}}e^{-}\left(\frac{4\ln 2(\mathrm{x}-\mathrm{x_0})^2}{\mathrm{w}^2}\right)\right\} \quad (1)$$

where I is the measured intensity, $\mathrm{I_0}$ is the background level, A is a constant, $\mathrm{x_0}$ the peak position, and w the full-width at half-maximum (FWHM). The crystallite sizes were then estimated from the reflections with the Scherrer formula:

$$L = \frac{0.9\lambda}{(\mathrm{w}\cos\theta)} \quad (2)$$

where λ is the wavelength of the X-rays used, and $2\theta \equiv \mathrm{x_0}$ is the peak position with w and θ in radians.

XRD spectra were taken pre and post testing to provide an indication of any structural changes (Fig.S11 and Fig.S12). Diffraction peaks are labelled with reference to those reported in the literature.[2,3] X-ray diffraction scans were collected over the $2(\theta)$ range 20^o to 70^o at a step size of 0.02^o with a copper X-ray source (λ=0.15419nm). The crystallite sizes of the metal oxide powders were found to be approximately 70 nm, remaining constant pre and post testing.

Further gas sensor testing results demonstrate the reproducibility of sensor responses after a cycle of testing at higher and lower operating temperatures. Fig.S13 displays the consistent response of the SWNT modified sensor to EtOH at 250 °C operating temperature before and after the sensor was operated at 300 °C. This suggests that the SWNT contribution to the sensing response is maintained after exposure to increased operating temperature. The

sensitivity of the SWNT composite sensor to humidity was also investigated (Fig.S14).

Digital photographs of the SWNT - metal oxide composite ink show the differences in ink colour (Fig.S17). The surfactant wrapped SWNT solution post sonication is shown in Fig. S18. An example of a sensor device in it's plastic casing is shown in Fig. S19. Table S1 highlights changes in the baseline resistances of the SWNT - composite sensors, differing by two orders of magnitude when compared with their plain metal oxide counterpart

References

(1) Dresselhaus, M. S.; Dresselhaus, G.; Saito, R.; Jorio, A. *Physics Reports* **2005**, *409*, 47.

(2) Indrea, E.; Bica, E.; Popovici, E.-J.; Suciu, R.-C.; Rosu, M. C.; Silipas, T.-D. *Revue Roumaine de Chimie* **2011**, *56*, 589.

(3) Stroppa, D. G.; Montoro, L. A.; Beltran, A.; Conti, T. G.; da Silva, R. O.; Andres, J.; Leite, E. R.; Ramirez, A. J. *Chemical Communications* **2011**, *47*, 3117.

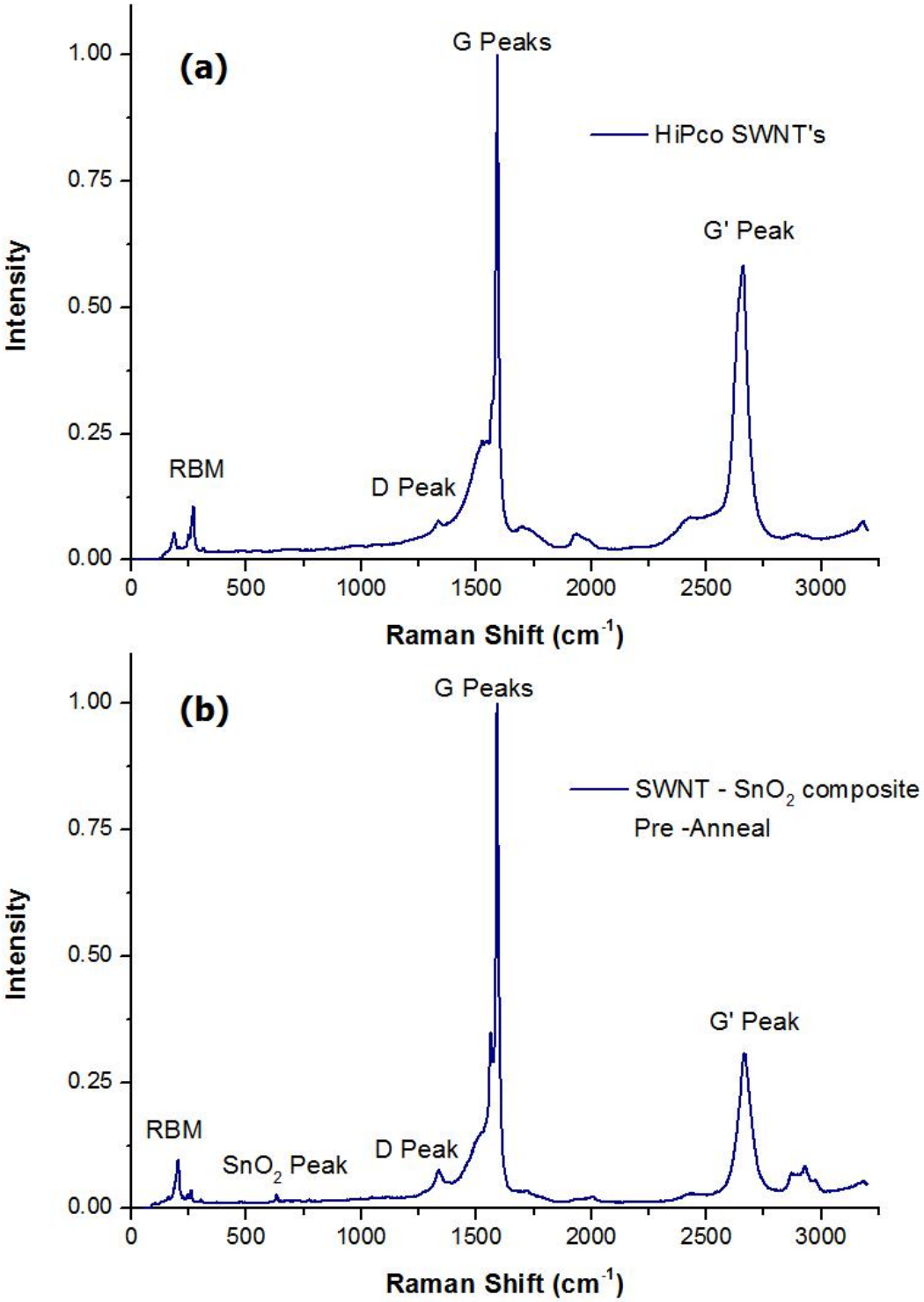

Figure S1: Raman spectra of (a) HiPco single-walled nanotubes wrapped in a solution of sodium deoxycholate (DOC) and heavy water (D_2O) and dried upon a glass substrate, (b) SWNT-SnO_2 composite in printed form on the sensor substrate pre annealing ($\lambda = 488$ nm)

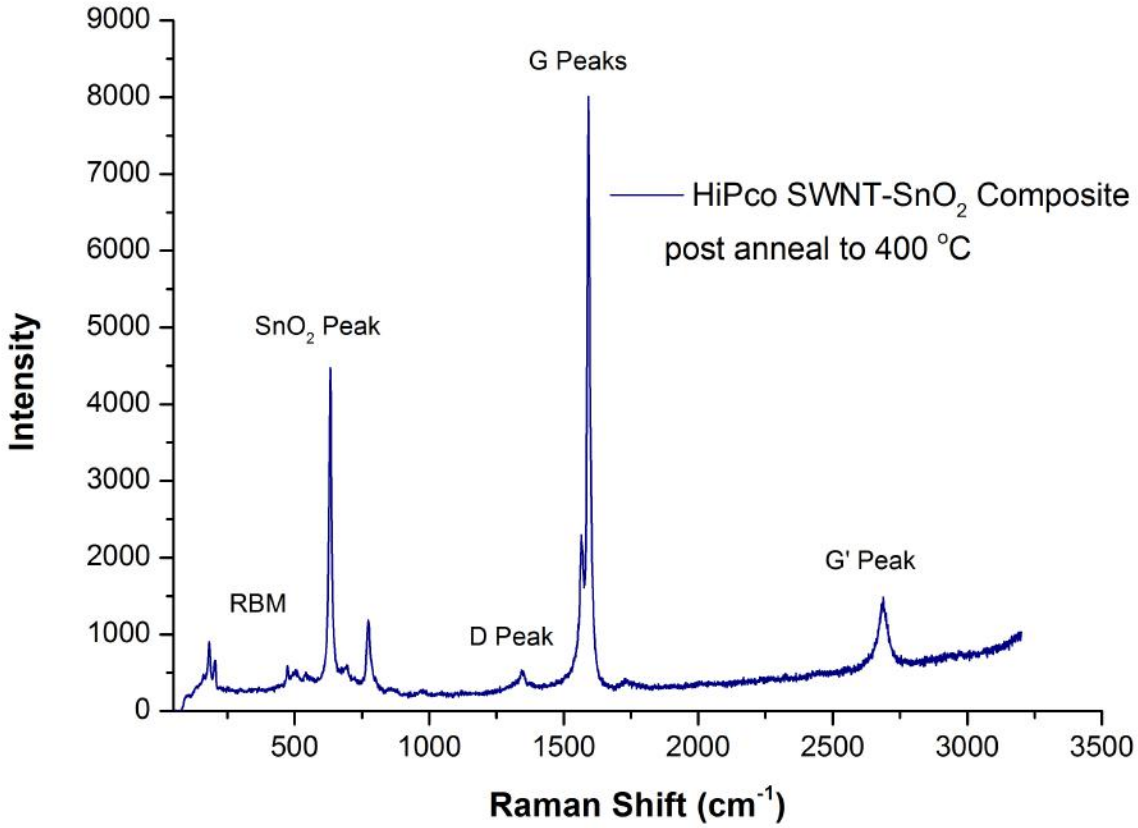

Figure S2: Raman spectrum of the SWNT-SnO_2 composite material post annealing to 400 °C

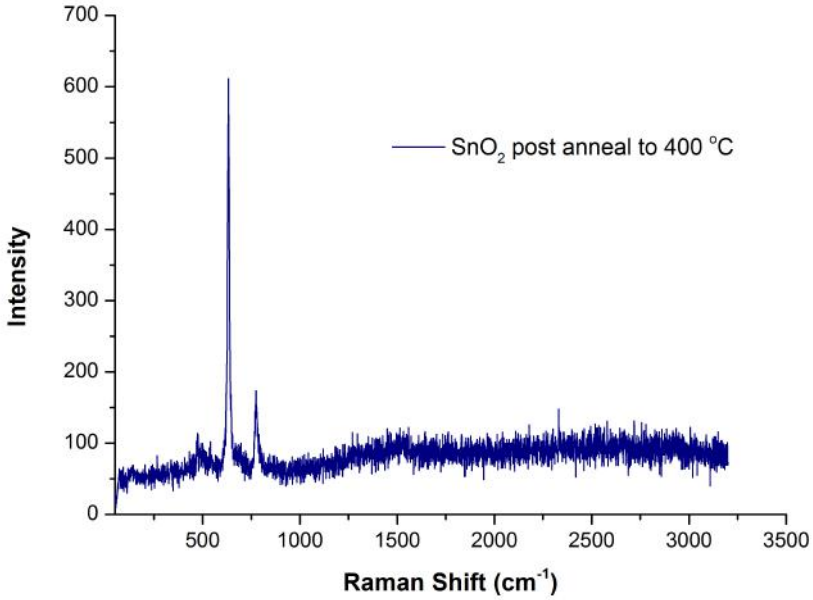

Figure S3: Raman spectrum of the SnO_2 composite material post annealing to 400 °C

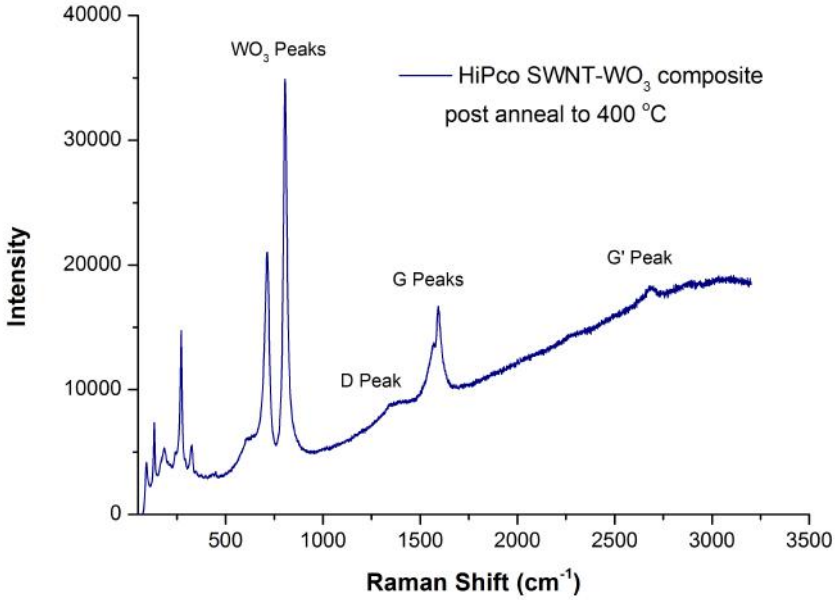

Figure S4: Raman spectrum of the SWNT-WO_3 composite material post annealing to 400 °C

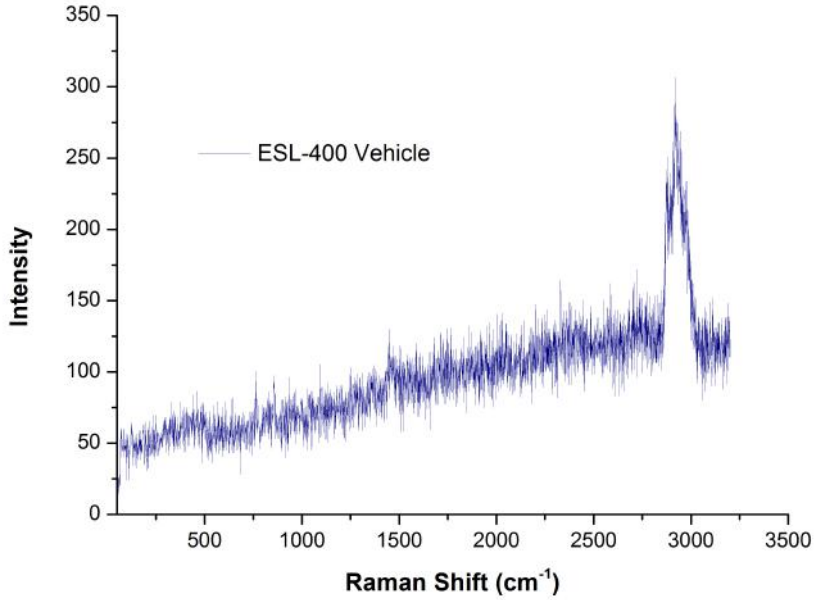

Figure S5: Raman spectrum of the ESL-400 vehicle pre annealing to 400 °C

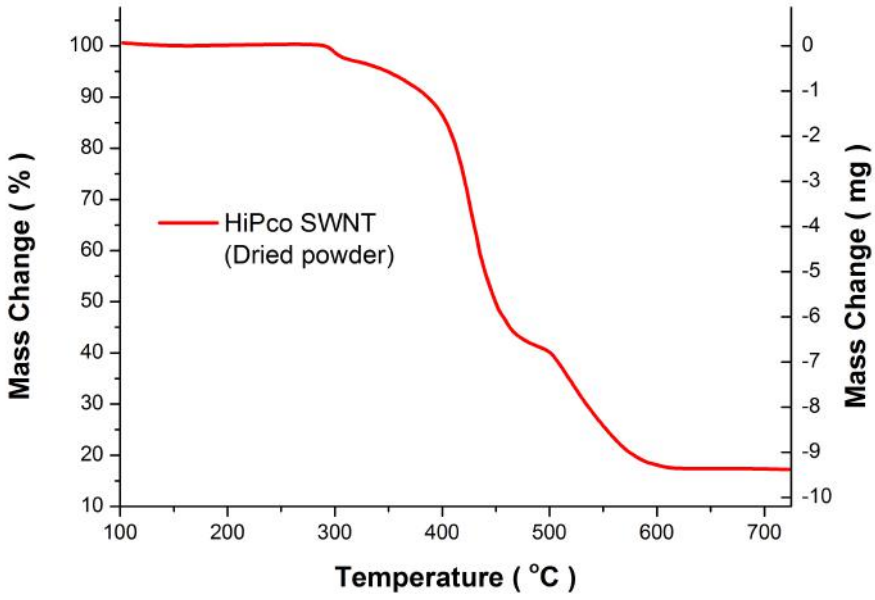

Figure S6: TGA profile of the HiPco SWNT's in dried powder form at a ramp rate of 5 °C per minute to 750 °C

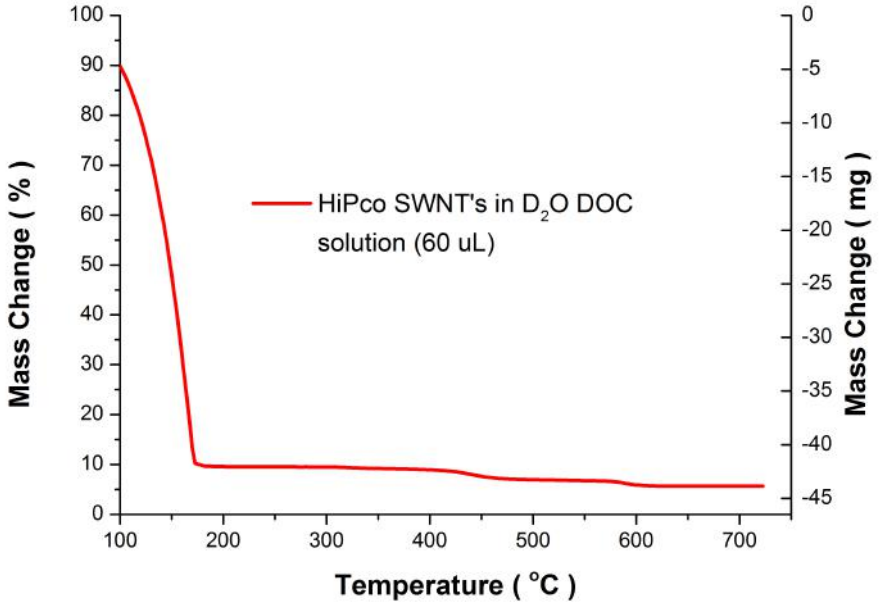

Figure S7: TGA profile of the surfactant wrapped HiPco SWNT's in D_2O DOC solution at a ramp rate of 15 °C per minute to 750 °C

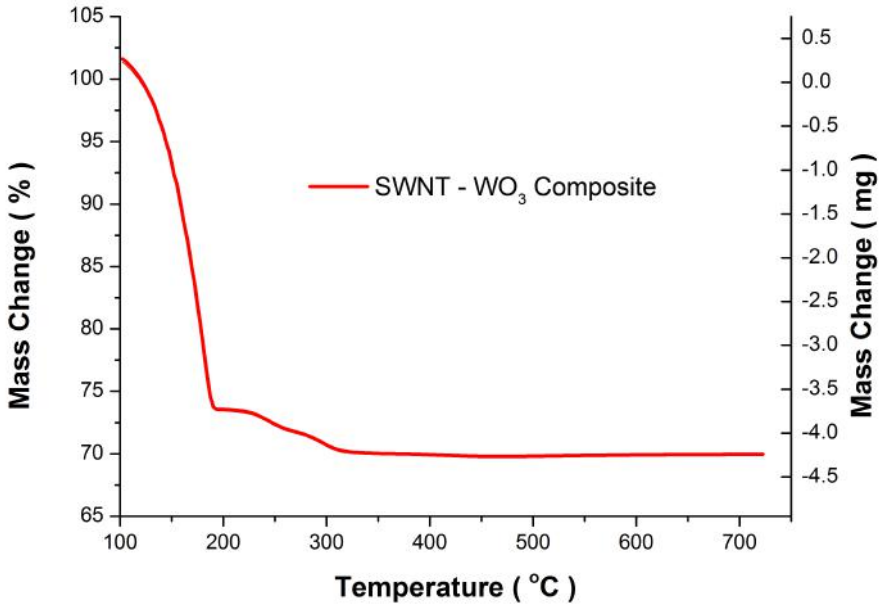

Figure S8: TGA profile of the SWNT - WO_3 composite at a ramp rate of 25 °C per minute to 750 °C

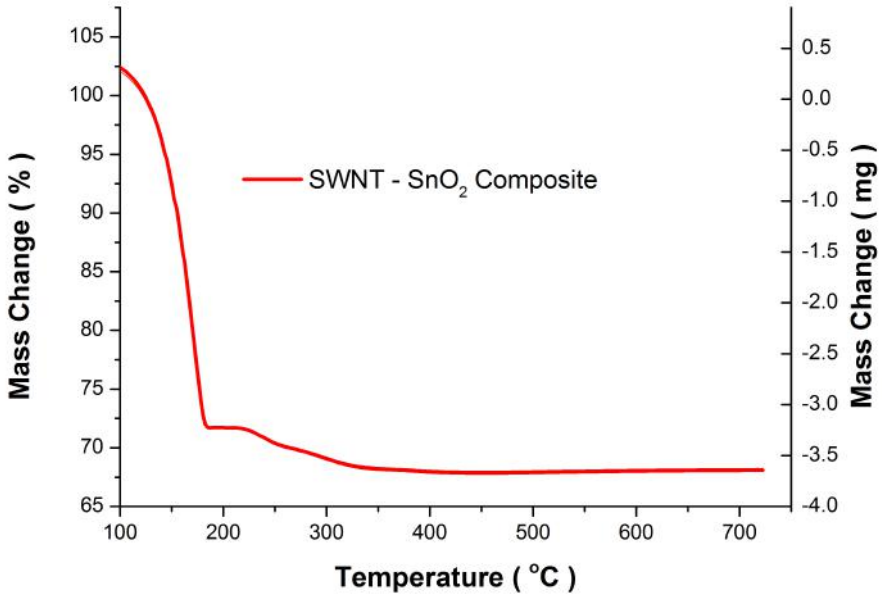

Figure S9: TGA profile of the SWNT - SnO_2 composite at a ramp rate of 25 °C per minute to 750 °C

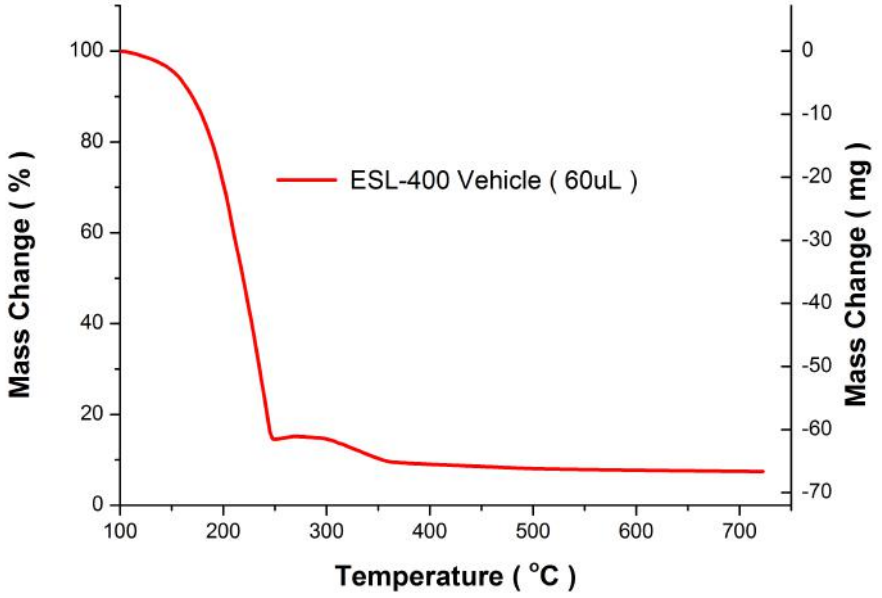

Figure S10: TGA profile of the ESL-400 vehicle at a ramp rate of 15 °C per minute to 750 °C

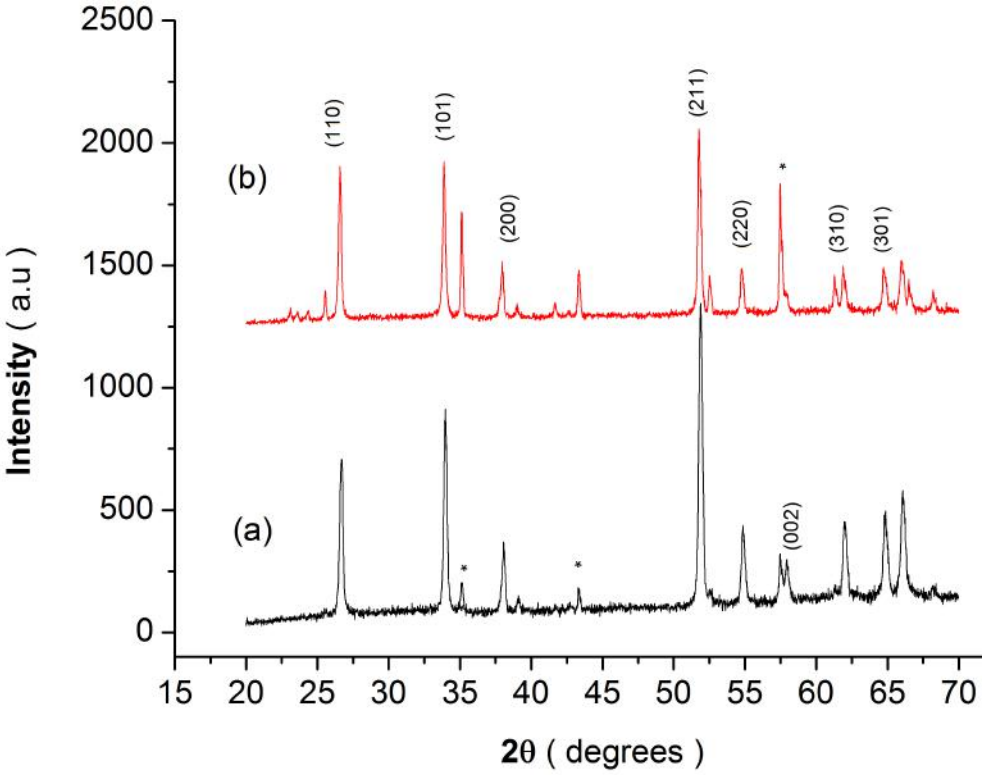

Figure S11: X-ray diffraction spectra for the SWNT-SnO_2 composite (a) pre testing (b) post testing. Peaks from the alumina substrate are highlighted with *

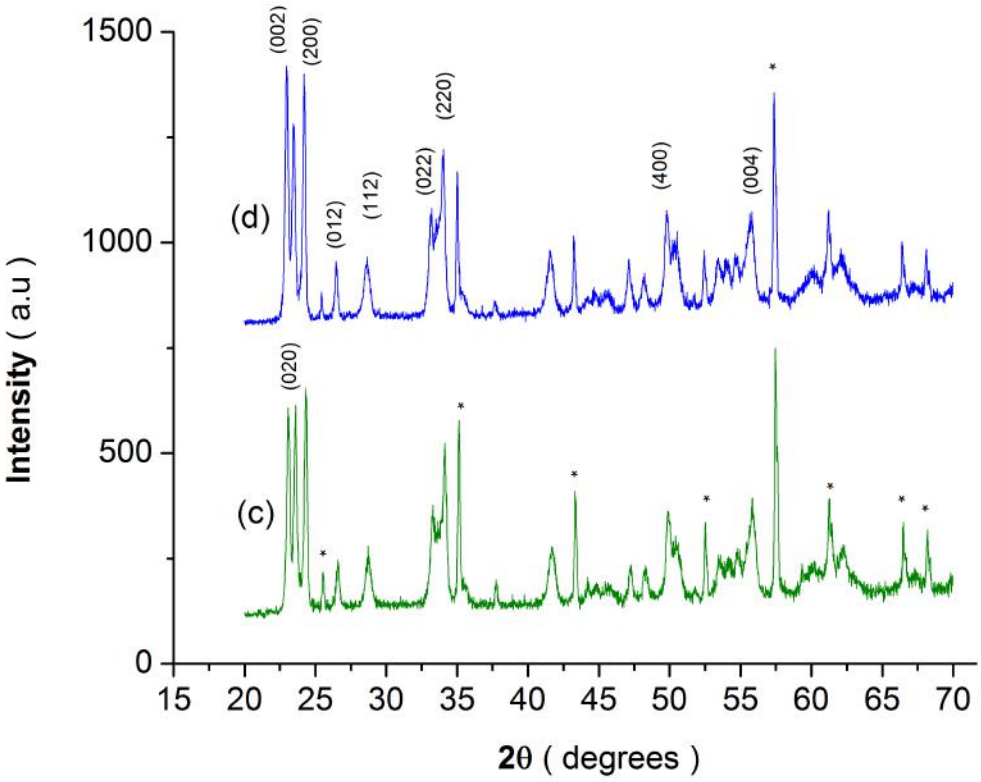

Figure S12: X-ray diffraction spectra for the SWNT-WO_3 composite (c) pre testing (d) post testing. Peaks from the alumina substrate are highlighted with *

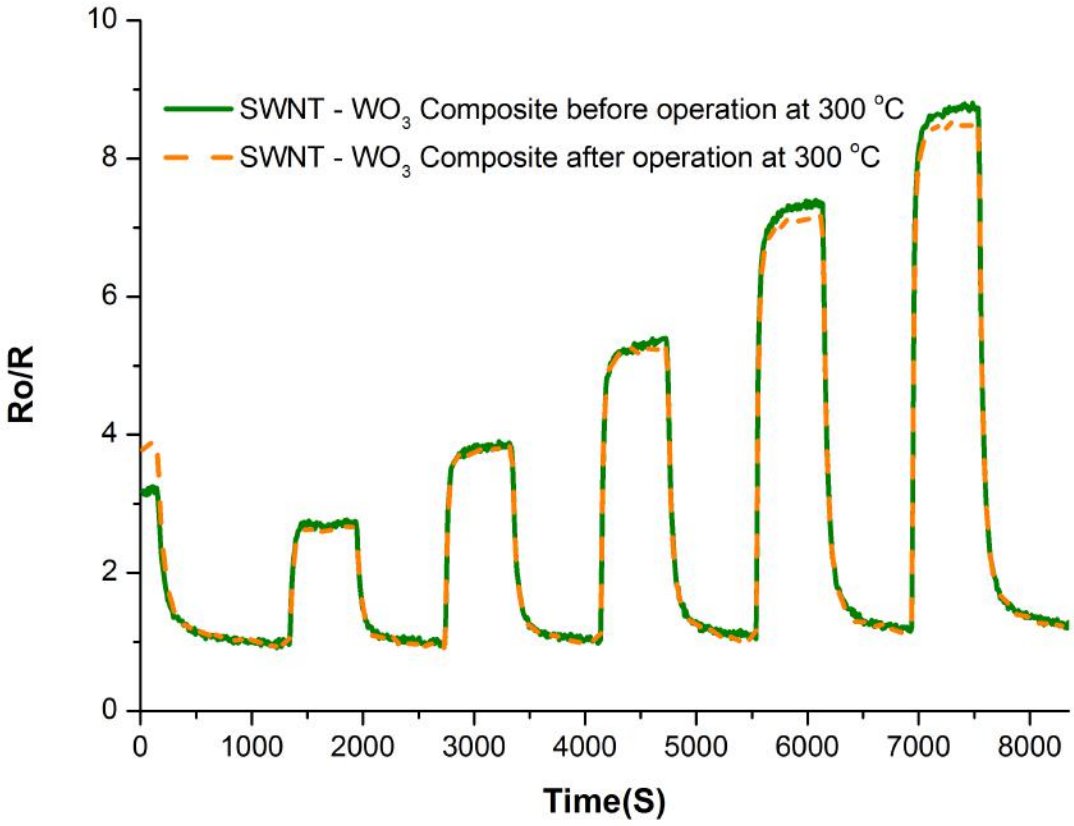

Figure S13: SWNT-WO_3 composite sensor response testing to ethanol at 250 °C before and after operation at 300 °C . Concentrations of 5, 10, 20, 40, 60 ppm

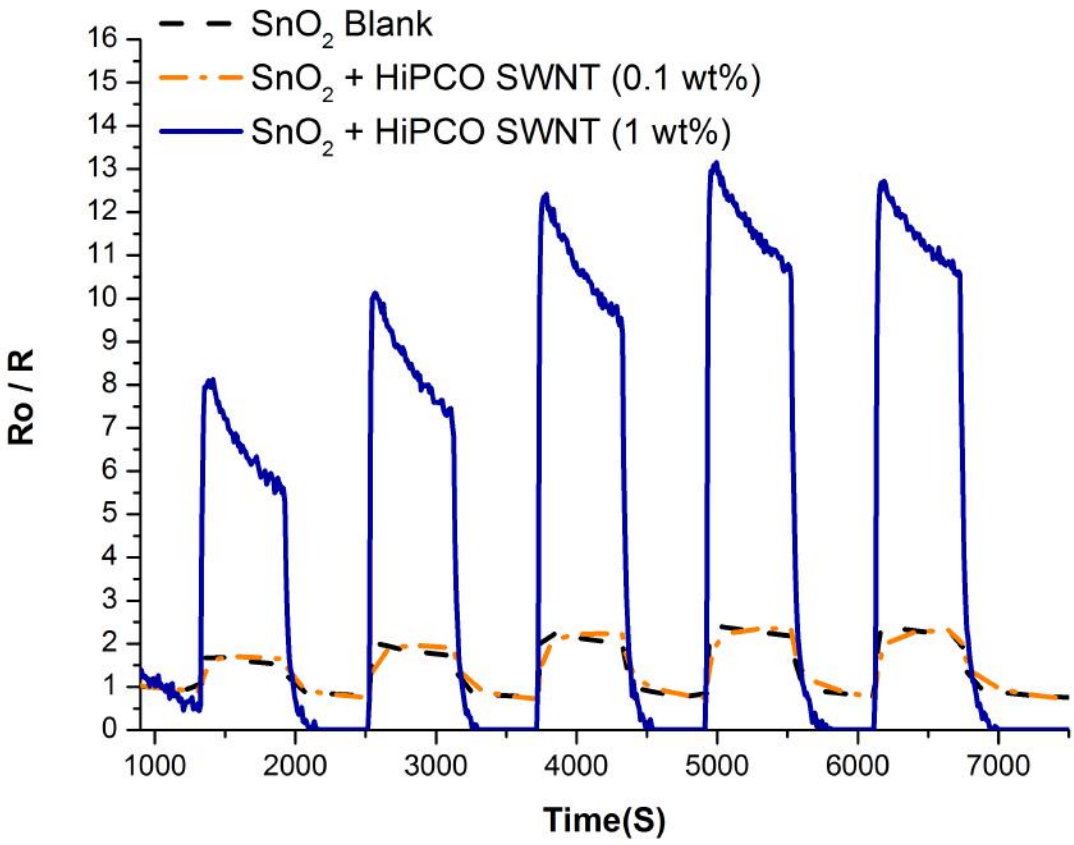

Figure S14: SWNT Blank and SWNT-WO_3 composite sensor sensitivity to humidity of 10%, 25%, 50%, 75% and 90% whilst operating at 250 °C

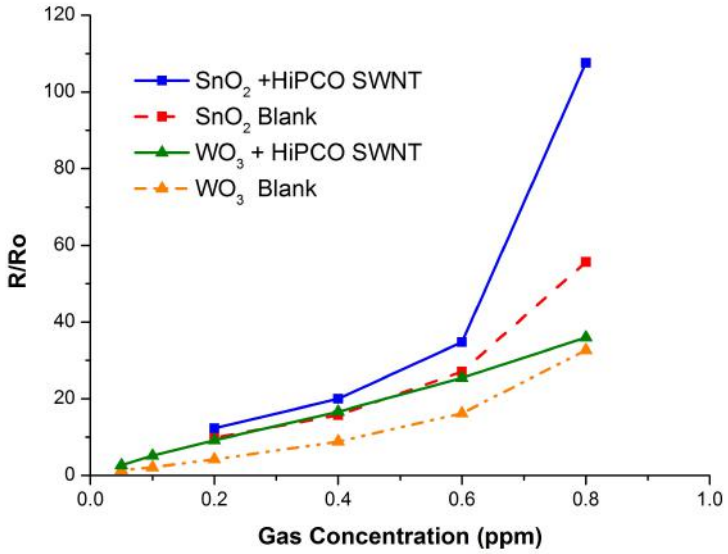

Figure S15: Varying WO_3 Blank, SWNT - WO_3 composite, SnO_2 Blank and SWNT - SnO_2 composite sensor responses as a function of increasing concentrations of NO_2 when operating at 250 °C.

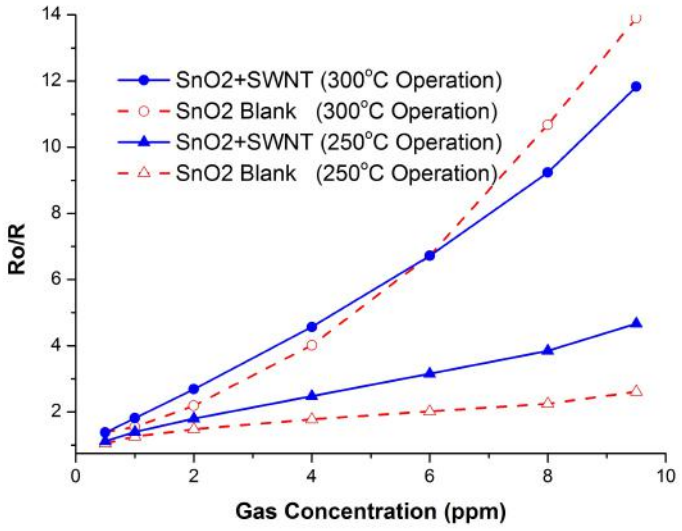

Figure S16: The effect of operating temperature (250 °C to 300 °C) on SWNT modified and blank SnO_2 device sensitivities as a function of Acetone concentration

Table S1: Sensor material, anneling temperature during fabrication and the sensor baseline resistance in air whilst operating at 250 °C

Sensor Material	Annealing Temperature (°C)	Baseline resistance in air (MΩ)
SnO_2 + Swnt	400	21
SnO_2	400	0.18
SnO_2	600	0.06
WO_3 + Swnt	400	5.8
WO_3	400	0.026

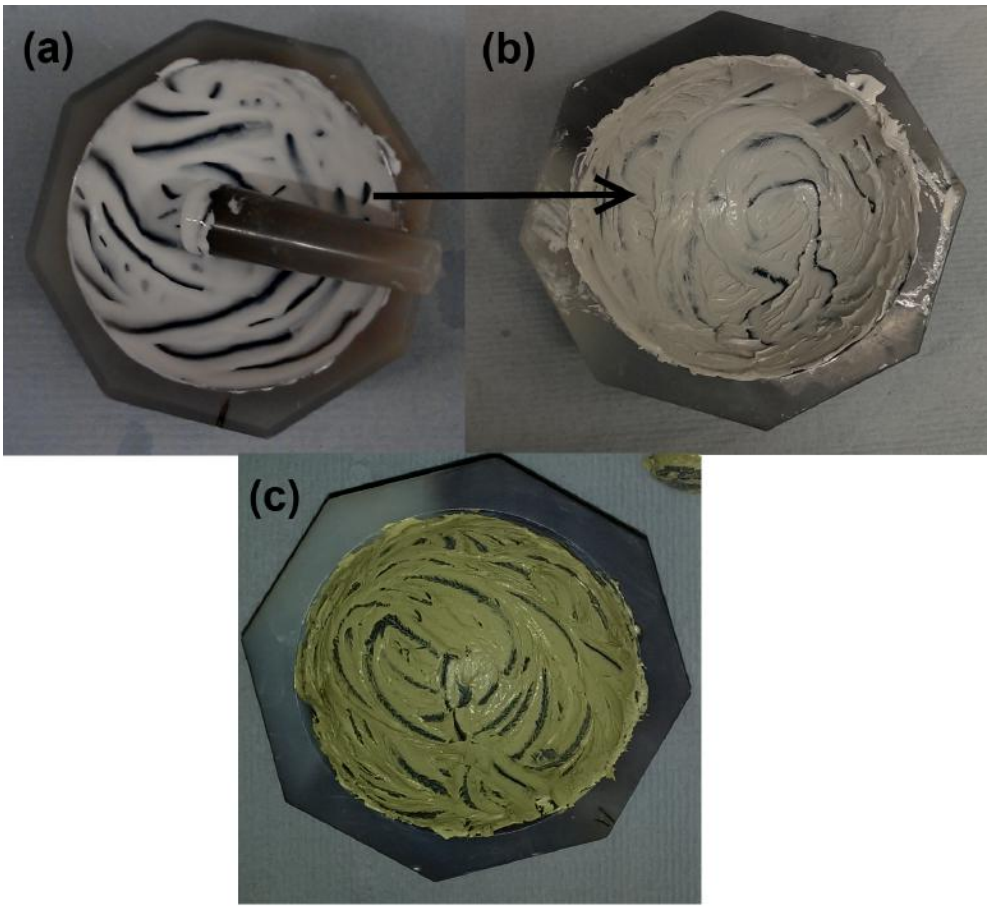

Figure S17: Ink colour change from (a) SnO_2 to (b) SWNT - SnO_2 composite ink after SWNT addition. (c) shows the SWNT - WO_3 composite ink

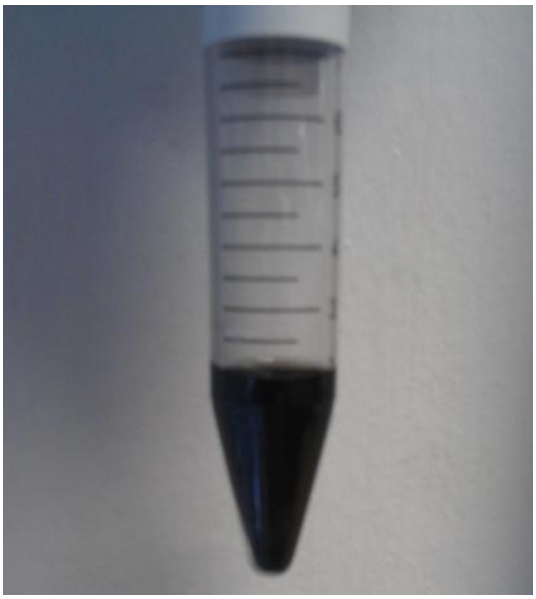

Figure S18: Surfactant (D_2O DOC) wrapped HiPco SWNT's post sonication

Figure S19: Final sensor device mounted onto plastic casing